



New active safety device dedicated to light all-terrain vehicle stability: Application to quad bike and off-road mobile robot

N. Bouton, R. Lenain, Benoît Thuilot, P. Martinet, M. Berducat

► To cite this version:

N. Bouton, R. Lenain, Benoît Thuilot, P. Martinet, M. Berducat. New active safety device dedicated to light all-terrain vehicle stability: Application to quad bike and off-road mobile robot. AgEng 2010, International Conference on Agricultural Engineering, Sep 2010, Clermont-Ferrand, France. 8 p., 2010. <hal-00525088>

HAL Id: hal-00525088

<https://hal.archives-ouvertes.fr/hal-00525088>

Submitted on 11 Oct 2010

HAL is a multi-disciplinary open access archive for the deposit and dissemination of scientific research documents, whether they are published or not. The documents may come from teaching and research institutions in France or abroad, or from public or private research centers.

L'archive ouverte pluridisciplinaire **HAL**, est destinée au dépôt et à la diffusion de documents scientifiques de niveau recherche, publiés ou non, émanant des établissements d'enseignement et de recherche français ou étrangers, des laboratoires publics ou privés.

New active safety device dedicated to light all-terrain vehicle stability: Application to quad bike and off-road mobile robot

N. Bouton¹, R. Lenain¹, B. Thuilot², P. Martinet², M. Berducat¹

¹ Cemagref – Unité TSCF, 24 av. des Landais, BP 50085, 63172 Aubière Cedex. France.

² LASMEA, 24 av. des Landais, 63177 Aubière Cedex. France.

Abstract

According to their specific geometric and dynamic characteristics (small weight, huge reachable speeds...), All-Terrain Vehicles (ATVs - as quad bikes) and off-road mobile robots are very compact and driveable. They permit to realize extra agricultural tasks (spreading, spraying...) in an easier way than using once more a heavy farm tractor. However such vehicles require highly accurate control laws, able to preserve their stability even at high speed.

In this paper, the prevention of off-road vehicle and mobile robot rollover are addressed by using a new active safety device. It consists in using Predictive Functional Control (PFC) so as to compute, on-line, the maximum vehicle velocity, compatible with a safe motion over some horizon of prediction, and can be applied, if needed, to the vehicle actuator to prevent from rollover. The capabilities of the proposed device are demonstrated and discussed thanks to both advanced simulations and real experimentation.

1. Introduction

Off-road mobile robots and light All-Terrain Vehicles (ATV) appear as an interesting solution so as to answer social needs in various fields of application ([1] - farming, surveillance, military activities, etc). However, if many potential devices can take benefits of innovation in this area (increasing work accuracy, decreasing the level of risk), such applications require highly accurate control laws, able to preserve vehicle stability even at high speed. Indeed, in off-road mobile robot context, the complexity and the variability of the encountered phenomena have to be tackled to ensure both accuracy and security. Nevertheless, if numerous systems have been developed for road vehicles (active suspensions, active steering [2], steering and braking control [3] and [2]), they appear to be poorly relevant for fast off-road motion context (since they do not adapt to varying grip conditions). Consequently, specific safety devices have to be designed for off-road mobile robots.

The first step in the development of such devices is the design of a rollover indicator dedicated to off-road mobile robots. Previous work [4] has shown that the Lateral Load Transfer (LLT - [5]) is a very relevant criterion. Its advantages, with respect to other stability metrics such as the Static Stability Factor (SSF) [6], the force-angle measurement criterion [7] or the Zero Moment Point (ZMP - proposed usually to investigate humanoid and mobile robot stability, [8]) are that, on the one hand it does not demand for a huge and expensive perception system, and on the other hand it is not dependent on some thresholds particularly difficult to tune in outdoor environment.

In order to use properly such a metric in an off-road context, grip conditions have to be known. A new observer has been proposed in [9]. It consists in the on-line adaptation of tire cornering stiffnesses, representative of grip conditions, based on a vehicle dynamic model. Then, using the adapted parameters, it permits to access the sideslip angles to be entered into the algorithms proposed in [10], so as to control robot motion with a high accuracy whatever ground conditions, vehicle velocity (up to 40km/h) and the shape of the path to be

followed. Thanks to the estimation of cornering stiffnesses, this observer appears also to be relevant in the on-line computation of the Lateral Load Transfer and finally for the design of stabilizing algorithms.

In this paper, this indicator is used as a basis for designing an active anti-rollover device dedicated to mobile robots. More precisely, the maximum vehicle velocity ensuring that the LLT remains within a safety range over the horizon of prediction is estimated on-line, and can then be applied to the vehicle actuator in order to avoid imminent rollover. The algorithm relies on Predictive Functional Control principle (PFC - [11], [12]), so that off-road mobile robot dynamic features can be accounted.

The paper is organized as follows: vehicle modeling in presence of slidings used to develop the control device is presented. Then, previous work on path tracking is recalled as well as the notion of *Mixed observer* used for the estimation of grip conditions (cornering stiffnesses) and sliding parameters (sideslip angles). Next, Predictive Functional Control principle is applied to design vehicle velocity control law in order to guarantee lateral dynamic stability of mobile robots on slippery ground. Finally, experimental results are reported to validate the relevancy of the proposed approach in situations where lateral rollover is imminent.

2. Vehicle modelling

2.1. Vehicle dynamic model

In order to describe the rollover of a mobile robot, its motion in yaw and roll representations has to be known. Then, two representations are here introduced: one is a yaw representation (Figure 1) (also used to develop the *Mixed observer* described in Section) and the other one is a roll representation (Figure 2). The yaw model, also used for path tracking and sliding estimation aims at describing the overall vehicle motion on the ground and consists of an extended bicycle model of the mobile robot. It is used to estimate some vehicle motion variables (as the lateral acceleration of the vehicle center of gravity) and sideslip angles. These variables are then injected into the second part of the dynamic model, characterized by a roll 2D projection (shown on Figure 2)), used to compute roll angle, roll rate and the LLT.

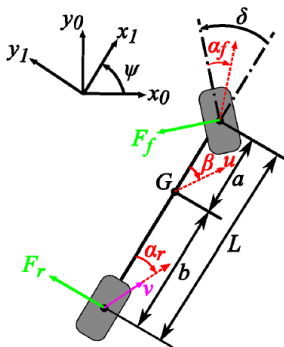


Figure 1 : Yaw projection of the dynamic model

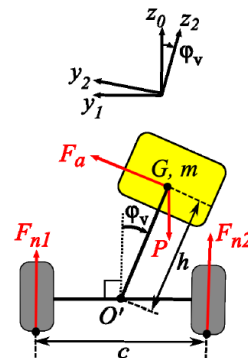


Figure 2: Roll projection of the dynamic model

Motion equations issued from the yaw projection shown in Figure 1 require analytical expressions of lateral forces F_f and F_r . Therefore, as explained in [13], a simple linear tire model has been considered. It can be expressed as:

$$\begin{cases} F_f = C_f(\cdot)\alpha_f \\ F_r = C_r(\cdot)\alpha_r \end{cases} \quad (\text{Eq.1})$$

This model requires only the knowledge of α_f and α_r and the front and rear cornering stiffnesses $C_f(\cdot)$ and $C_r(\cdot)$ supposed to be slow varying. In order to reflect the variable grip conditions, these two parameters are on-line estimated thanks to the *Mixed observer* detailed in Section . Only one parameter is then needed, contrary to classical tire models such as the celebrated Magic formula [14].

2.2. LLT definition

The general expression of the Lateral Load Transfer (LLT) (see [15]) is:

$$LLT = \frac{F_{n1} - F_{n2}}{F_{n1} + F_{n2}} \quad (\text{Eq.2})$$

Clearly, a rollover situation is detected when a unitary value of $|LLT|$ is reached, since it corresponds to the lift-off of the wheels on the same side of the vehicle. Here, the vehicle behavior will be considered as hazardous when LLT reaches the critical threshold LLT_{limit} ($|LLT| > LLT_{\text{limit}}$).

2.3. LLT dynamic equation

In order to extract normal force expressions from the roll model (see Figure 2), the following assumptions have been made:

- The entire vehicle mass is suspended, which implies insignificant non-suspended mass (essentially tires),
- The suspended mass is assumed to be symmetrical with respect to the two planes (z_2, y_2) and (x_2, z_2). The inertial matrix is then diagonal in the roll frame $R_2(x_2, y_2, z_2)$,
- Sideslip angles β , α_f and α_r are assumed to be small (corroborated by experiments),
- As a consequence, the vehicle velocity u at roll center can be considered to be equal to the rear axle one (i.e. $u \approx v$).

Using these assumptions, the LLT indicator can be evaluated from the Newton Euler formalism applied to the overall system. More precisely, variations of the roll angle φ_v , and normal forces F_{n1} and F_{n2} can be derived as:

$$\ddot{\varphi}_v = \frac{1}{hc \alpha_v} \left[h \dot{\varphi}_v^2 \sin(\varphi_v) + (h \dot{\varphi}_v^2 \sin(\varphi_v)) + (u \dot{\varphi}_v \cos(\varphi_v)) \dot{\varphi}_v \sin(\varphi_v) + (u \dot{\varphi}_v \cos(\varphi_v)) \dot{\varphi}_v \sin(\varphi_v) + \left(\frac{k_r \varphi_v + b_r \dot{\varphi}_v}{m h} \right) c \alpha_v \right] \quad (\text{Eq.3})$$

$$(F_{n1} + F_{n2}) = m \left[-h \ddot{\varphi}_v \sin(\varphi_v) - h \dot{\varphi}_v^2 \cos(\varphi_v) + g - \left(\frac{k_r \varphi_v + b_r \dot{\varphi}_v}{mh} \right) \sin(\varphi_v) \right] \quad (\text{Eq.4})$$

$$(F_{n1} - F_{n2}) = \frac{2}{c} \left[I_x \ddot{\varphi}_v + (I_z - I_y) (\dot{\psi}^2 \cos(\varphi_v) \sin(\varphi_v)) - h \sin(\varphi_v) (F_{n1} + F_{n2}) \right] \quad (\text{Eq.5})$$

In order to infer the roll angle and the LLT from (4)-(5), the global sideslip angle and the yaw rate are both required. Since the former one cannot be measured, an observer has been designed and is presented below.

3. Mixed observer

As explained in the previous paragraph, both the dynamic modeling used to compute LLT and the path tracking algorithm require an estimation of sliding parameters. Then, an indirect estimation of dynamic model parameters is mandatory. Since appropriate sensors are missing, this is achieved in several steps, using different level of modeling (kinematic and dynamic). This multilevel estimation is gathered in the so called *Mixed observer* detailed in [9]. Its general principle is described in Figure 3. The observation loop consists of successive steps, each one relying on the variable supplied by the preceding step. The three blocks shown in Figure 3 are described below:

- A preliminary extended kinematic observer (red dashed box) is first used to supply relevant tire sideslip angle estimation at low speed.

- Then, the parameters obtained by the kinematic observer are used in the cornering stiffness observer (green dotted box) where the cornering stiffnesses are on-line adapted with the aim of reflecting grip condition variations.
 - Finally, with the adapted parameters, a dynamic sideslip angle observer (blue dashed dotted box), derived from standard observer theory, is applied in order to get relevant sideslip angles estimation at high speed and whatever the grip conditions.
- The sliding angle estimates supplied by such an observer are relevant to compute LLT and to develop anti-rollover predictive control laws as detailed below.



Figure 3 : Scheme of the path tracking controller

4. Predictive functional control of the vehicle

In order to avoid the rollover risk, the limitation of the LLT (i.e. $LLT \leq \text{critical threshold value}$ – here, $LLT \leq 0.8$) through the control of the ATV speed is here investigated. The idea is to compute at each time the velocity leading to this LLT threshold one moment in the future. This value can then be considered as the maximum admissible velocity (denoted v_{max} in the sequel) to avoid lateral rollover situation.

The global scheme is depicted on the following figure:

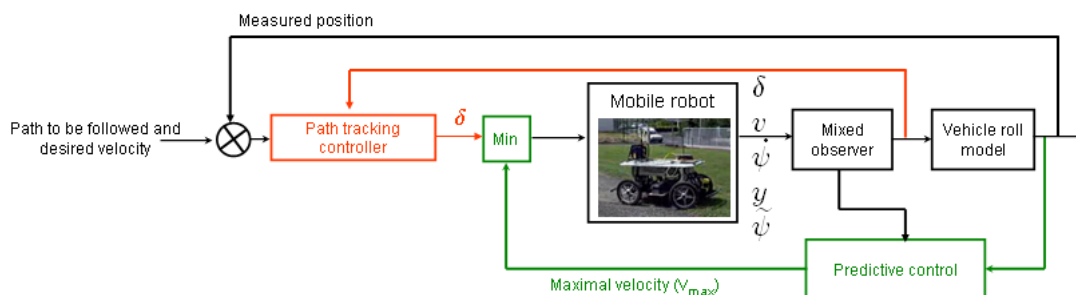


Figure 4 : Predictive velocity control of an ATV

The computation of the maximum velocity, detailed is represented by the block "Predictive control". Relying on this variable, the speed limitation process consists on the following steps:

1. The "Min" block supplies the rear axle linear velocity control input v_{input} to be applied to the vehicle. This variable is deduced from the comparison between the velocity specified by the pilot (or desired in the case of autonomous off-road mobile robot) v_{pilot} and the maximum velocity v_{max} : $v_{input} = \min(v_{pilot}, v_{max})$
2. The measurements shown in Figure 4 are then used to estimate on-line the sliding parameters and the cornering stiffnesses thanks to the *Mixed observer* described in Section ,

3. Then, stiffnesses (from the *Mixed observer*), the measured rear axle linear velocity and the measured steering angle are reported into the vehicle roll model in order to compute the roll angle ϕ and the LLT (see Section),

4. Finally, the roll angle ϕ , the sliding parameters and the steering angle are processed in the "Predictive Control" block in order to supply the maximum velocity v_{max} .

In order to anticipate (and then avoid) hazardous situations, the computation of v_{max} is based on the Predictive Functional Control (PFC) formalism, detailed in [11] and [12] by using the roll angle evolution supplied by (3). The vehicle velocity is then viewed as a control variable and v_{max} is designed in order to ensure the convergence of the LLT to the value 0.8.

5. Results

5.1. Advanced simulation

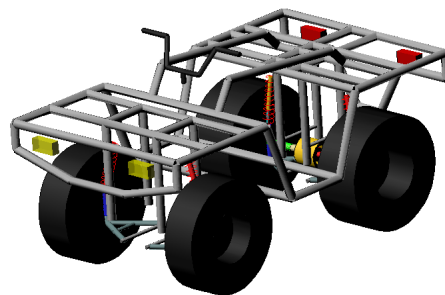


Figure 5: Virtual quad bike

An advanced simulation has been done with the virtual quad bike described on Figure 5, where rear axle linear velocity control strategy has been applied. The velocity and steering angle specified by the pilot during the simulation are depicted on Figure 6.

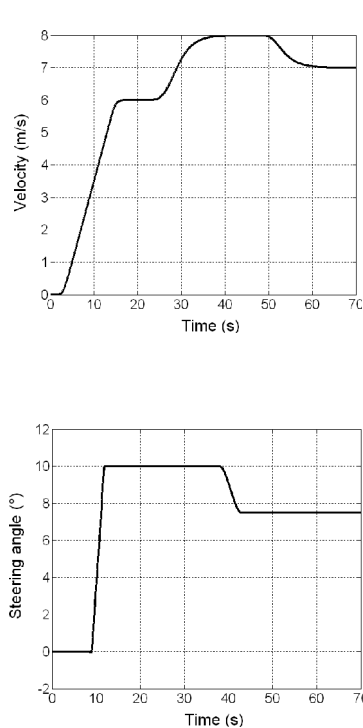


Figure 6: Pilot desired velocity and steering angle

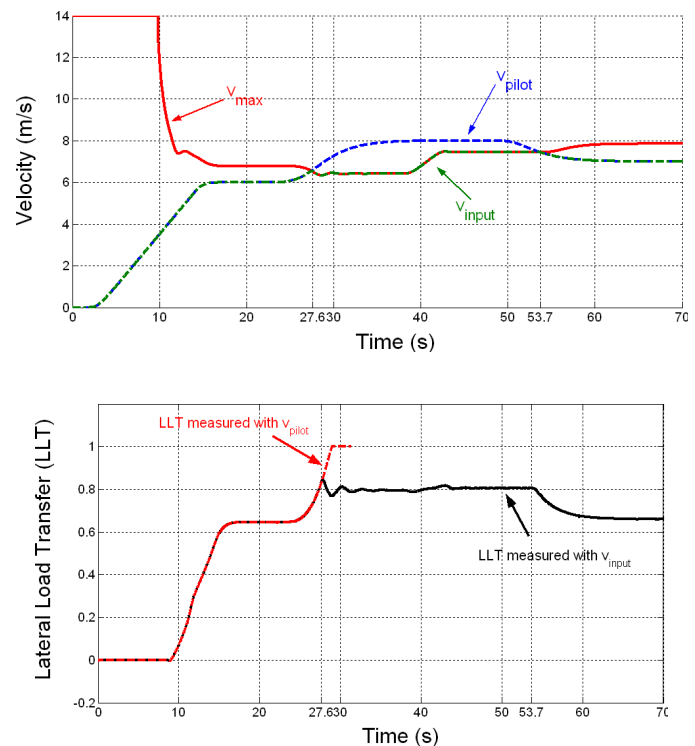


Figure 7: Velocity control and Lateral Load Transfer results

Figure 7 shows the time evolution of the velocity specified by the pilot v_{pilot} (in blue dash-dotted line), the maximum velocity v_{max} (computed with the PFC algorithm, in red solid line)

and the rear axle velocity v_{input} to be applied to the vehicle (in green dashed line). From $t=0s$ to $t=10s$, the virtual quad bike is either moving according to a straight line or the steering angle value is low ($\delta < 3^\circ$). Therefore the maximum velocity cannot be computed and is then set to 14m/s. After $t=10s$, the velocity to be applied v_{input} is equal to the minimum of v_{pilot} and v_{max} . As a result, first, v_{input} is equal to v_{pilot} , then, between $t=27.6s$ and $t=53.7s$, $v_{input} = v_{max}$, because v_{pilot} is too high with respect to the steering angle values, even when the steering angle is decreased from 10° to 7.5° . Finally, after $t=53.7s$, v_{pilot} has been reduced, so that v_{pilot} can again be actually applied.

Figure 7 also shows the time evolution of the LLT measured on the virtual quad bike when respectively v_{input} (black solid line) and v_{pilot} (red dashed line) are applied. In the last case, after $t = 29s$, the vehicle rollovers (since $LLT = 1$). Contrarily, when v_{input} is applied, the LLT safely converges to the LLT threshold value ($LLT = 0.8$) when v_{pilot} exceeds v_{max} . Vehicle rollover has then satisfactorily be avoided, while keeping vehicle velocity as high as possible in such a situation.

5.2. Real experiment

A real experiment has been performed with the robot described in Figure 8. It consists of an electric off-road vehicle. The main exteroceptive sensor on board is a Dassault-Sercel dual frequency "Aquarius 5002" RTK-GPS receiver, which can supply an absolute position accurate to within 2cm, at a 10Hz sampling frequency. In addition, a gyrometer supplying a yaw rate measurement accurate to within $0.1^\circ/s$ is fixed on the chassis as well as a steering angle sensor and a Doppler radar.



Figure 8 : Experimental platform

Then, two tests have been performed: the first one consists in using path tracking control without predictive control and a constant $v_{pilot}=v_d=6m/s$ velocity. The second test consists in using the predictive functional control algorithm dedicated to LLT limitation and $LLT_{limit}=0.35$.

Figure 9 shows the time evolution of the measured velocity v_{m1} when path tracking is done without velocity control ($v_{m1} \approx v_d \approx 6m/s$ after settling time) in black dash-dotted line, the maximum velocity v_{max} (computed with the PFC algorithm, in red solid line) and the rear axle velocity v_{m2} measured on the vehicle (in green dashed line) when velocity control is used. As described in Section , v_{m2} is supposed to be equal to the minimum of v_d and v_{max} . From $t=0s$ to $t=5.8s$, v_{m2} is equal to v_d . Then, between $t=5.8s$ to $t=9.2s$, during the curved part of the reference path, the velocity control variable applied to the vehicle is the maximum velocity given by the predictive functional control algorithm. However, due to the delay introduced by the velocity actuator, the measured velocity v_{m2} is satisfactorily superposed with v_{max} only beyond $t=7.8s$. Finally, after $t=9.8s$, v_{max} is superior to the desired velocity, so that v_d can again be actually applied and after settling time ($t=13s$), the measured velocity v_{m2} converges to v_d .

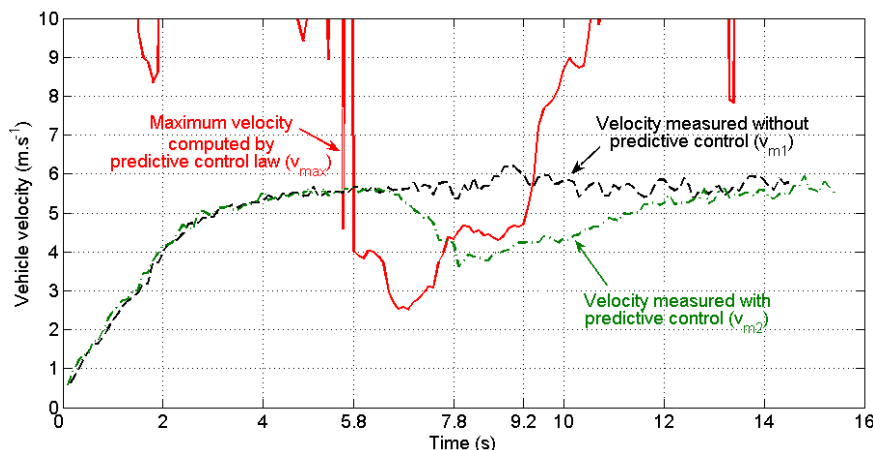


Figure 9 : Velocities comparison during real experiment

Figure 10 shows the time evolution of the Lateral Load Transfer of the vehicle. LLT without prediction (LLT obtained when $v_{m1} \approx v_d$ is measured on the vehicle) is depicted in black dash-dotted line and the LLT measured with the predictive control is depicted in red solid line (LLT obtained with v_{m2} , i.e. when the minimum of v_d and v_{max} is applied to the vehicle). In this figure, the LLT obtained with v_{m1} is largely superior to LLT_{limit} fixed here at 0.35. On the contrary, after the settling time (after $t=8s$), the LLT measured with v_{m2} satisfactorily converges to the LLT_{limit} . Indeed, between $t=6s$ and $t=8s$, the LLT measured is superior to the LLT_{limit} , since the velocity actuator introduces a delay between the velocity control variable, here equal to the maximum velocity v_{max} computed via PFC algorithm and the real velocity of the vehicle v_{m2} , as explained in the previous paragraph and which can be seen on Figure 9. Finally, when $v_{m2} \approx v_{max}$, the LLT measured is equal to 0.35.

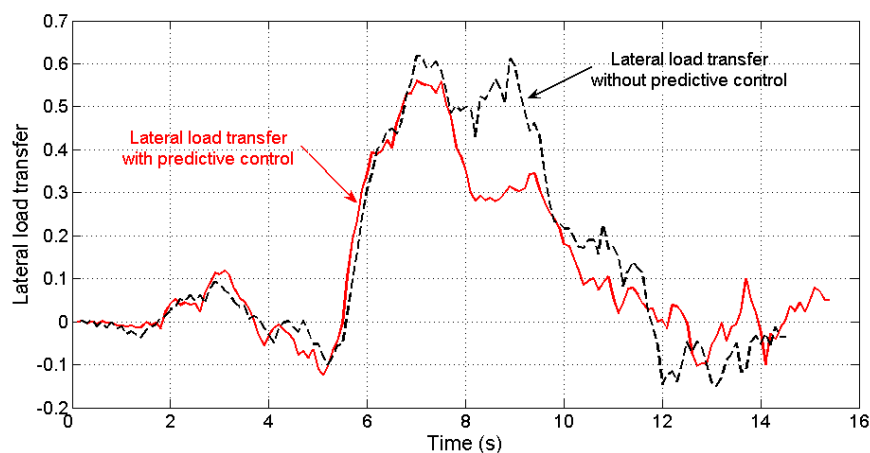


Figure 10 : Lateral Load Transfer measured

6. Conclusion

This paper proposes a new safety device, based on Predictive Functional Control formalism, dedicated to off-road mobile robots operating on a natural and slippery ground. First, previous work on path tracking control, built from both adaptive and predictive control laws, has been recalled. Sliding effects have been taken into account according to a mixed kinematic and dynamic observer adapting on-line the tire cornering stiffnesses of the front and rear tires. It enables to take into account the non-linear behavior of the tire and the variations in grip conditions when computing the sideslip angles. Then, these sliding parameters are introduced into a predictive functional control law, based on a vehicle dynamic model, so as to compute the maximum velocity admissible by the robot, ensuring

that the LLT indicator never exceeds the rollover threshold (i.e. $|LLT| < LLT_{limit}$). Real experiments, carried out with a high speed mobile robot, demonstrate the applicability and the relevancy of the proposed control strategy to avoid rollover situations and ensure path tracking trajectory.

Future work will be dedicated to reduce the delay introduced by the velocity actuator. Indeed, it has been highlighted that the velocity measured on the vehicle differs from the velocity control variable. Therefore, another predictive control law based on the velocity actuator characteristics is under development so as to eliminate the delay.

References

1. Siegwart, R. and I.R. Nourbakhsh, "Introduction to autonomous mobile robots". MIT Press, Vol. 2004.
2. Bosch, R., "Safety, comfort and convenience systems". Wiley. Hoboken, U.S.A., 2006.
3. Ackermann, J. and D. Odenthal. "Advantages of active steering for vehicle dynamics control", in International Conference on Advances in Vehicle Control and Safety. Amiens: France. 1998.
4. Bouton, N., R. Lenain, B. Thuilot and P. Martinet. "An active anti-rollover device based on predictive functional control : Application to an All-Terrain Vehicle", in Int. Conf. on Robotics and Automation (ICRA). Kobe, Japan. 2009.
5. Gaspar, P., Z. Szabo and J. Bokor. "The design of an integrated control system in heavy vehicles based on an LPV method", in 44th IEEE Conf. on Decision and Control (CDC). Seville, Spain. 2005.
6. National Highway Traffic Safety Administration (NHTSA). "Trends in static stability factor of passenger cars, light trucks and vans". U.S. department of transportation. Springfield, U.S.A. 2005
7. Papadopoulos, E.G. and D.A. Rey. "A new measure of tipover stability margin for mobile manipulators", in Intern. Conf. on Robotics and Automation. Minneapolis, U.S.A. 1996.
8. Sardain, P. and G. Bessonnet, "Forces acting on a biped robot. Center of pressure - Zero moment point". IEEE Transactions on systems, man, and cybernetics, Vol. 34, pp.630-637, 2004.
9. Lenain, R., B. Thuilot, C. Cariou and P. Martinet. "Multi-model based sideslip angle observer : Accurate control of high-speed mobile robots in off-road conditions", in Int. Conf. on Intelligent Robots and Systems (IROS). Saint Louis, U.S.A. 2009.
10. Lenain, R. "Contribution à la modélisation et à la commande de robots mobiles en présence de glissement". Ph.D. thesis. Université Blaise Pascal, Clermont II, 2005.
11. Richalet, J., E. Abu, C. Arber, H. Kuntze, A. Jacubasch and W. Schill. "Predictive functional control - application to fast and accurate robots", in 10th IFAC World Congress. Munich, Germany. 1997.
12. Vivas, A. and V. Mosquera. "Predictive functional control of a {PUMA} robot", in Proc. of the first ICGST International Conference on Automatic Control and Systems Engineering (ACSE). Cairo, Egypt. 2005.
13. Bouton, N., R. Lenain, B. Thuilot and P. Martinet. "A rollover indicator based on a tire stiffness backstepping observer : Application to an All-terrain vehicle", in Int. Conf. on Intelligent Robots and Systems (IROS). Nice, France. 2008.
14. Pacejka, H. B., "Tire and vehicle dynamics". Society of Automotive Engineers. 2002.
15. Miège, A.J.P. and D. Cebon. "Design and implementation of an active roll control system for heavy vehicles", in 6th Int. symposium on Advanced Vehicle Control (AVEC). Hiroshima, Japon. 2002.